NEW SINGLE-YEAR RADIOCARBON MEASUREMENTS BASED ON DANISH OAK COVERING THE PERIODS AD 692–790 AND 966–1057

Sabrina G K Kudsk[1] • Bente Philippsen[2,3] • Claudia Baittinger[4] •
Alexandra Fogtmann-Schulz[1] • Mads F Knudsen[1] • Christoffer Karoff[1,5] •
Jesper Olsen[2,3]*

[1]Institute for Geoscience, Aarhus University, Høegh-Guldbergs Gade 2, DK-8000 Aarhus C, Denmark
[2]Aarhus AMS Centre (AARAMS), Department of Physics and Astronomy, Aarhus University, Ny Munkegade 120, DK-8000 Aarhus C, Denmark
[3]Centre for Urban Networks Evolutions (UrbNet), Aarhus University, Moesgård Allé 20, DK-8270 Højbjerg, Denmark
[4]Environmental Archaeology and Materials Science, National Museum of Denmark, IC Modewegs Vej, Brede, DK-2800 Kgs. Lyngby, Denmark
[5]Stellar Astrophysics Centre, Department of Physics and Astronomy, Aarhus University, Ny Munkegade 120, DK-8000 Aarhus C, Denmark

ABSTRACT. Single-year measurements of radiocarbon (^{14}C) in tree rings have led to the discovery of rapid cosmic-ray events as well as longer lasting anomalies, which have given new insights into the Sun's behavior in the past. Here, we present two new single-year ^{14}C records based on Danish oak that span the periods AD 692–790 and 966–1057, respectively, and consequently include the two rapid cosmic-ray events in AD 775 and 994. The new data are presented along with relevant information on the dendrochronological dating of the wood pieces, implying that these new measurements may contribute towards generating the next international calibration curve. The new data covering the AD 966–1057 period suggest that the increase in atmospheric ^{14}C associated with the cosmic-ray event in AD 994 actually occurred in AD 993, i.e. one year earlier than the year reported in Fogtmann-Schulz et al. (2017) based on oak from southern Denmark. Careful reanalysis of the dendrochronology that underpins the new ^{14}C records based on oak material from southern Denmark reveals that the cosmic-ray event reported in Fogtmann-Schulz et al. (2017) actually took place in AD 993.

KEYWORDS: annual data, calibration curve, radiocarbon dating, tree rings.

INTRODUCTION

As part of an effort to enhance the time resolution of the present international calibration curve (IntCal13, Reimer et al. 2013), and to increase the potential for investigating detailed changes in past solar activity, a substantial amount of single-year tree ring radiocarbon (^{14}C) measurements have recently been produced (e.g. Jacobsson et al. 2017; Miyake et al. 2017b; Sakamoto et al. 2017; Marshall et al. 2018). New annual ^{14}C data are important since these give new insights into both the short- and long-term solar behavior, which are important to unraveling the processes governing the solar dynamo and to better understanding the link between solar variability and Earth's climate (Gray et al. 2010). Equally important, annual ^{14}C data will refine the present calibration curve by providing more detailed structure to the curve itself, which, in turn, will provide new possibilities for high-precision dating of various materials, such as the ^{14}C age calibration of archaeological artifacts (e.g. Pearson et al. 2018). Hence, it is of great importance that new tree-ring data submitted for future calibration curves are of sufficient quality in terms of the robustness of the dendrochronological age constraints, internal and external validation of ^{14}C measurements within each laboratory, and that the new ^{14}C ages are compared with existing ^{14}C data in order to ensure the calibrated ages are reliable and accurate. Furthermore, annual ^{14}C data have contributed to the findings of so-called solar cosmic-ray events, which are characterized by an abrupt increase in the amount of ^{14}C in Earth's atmosphere for one or several years (Miyake et al. 2012, 2013, 2014, 2017a; Usoskin et al. 2013; Jull et al. 2014, 2018; Wacker et al. 2014; Güttler et al. 2015; Rakowski et al. 2015; Fogtmann-Schulz et al. 2017; Wang et al. 2017; Park et al. 2017). Annually resolved ^{14}C

---

*Corresponding author. Email: jesper.olsen@phys.au.dk.

records have also been used to search for similar excursions in the atmospheric ^{14}C content that may be caused by near-Earth supernova explosions, but so far no clear indications of such an event have been found (Damon et al. 1995; Menjo et al. 2005; Dee et al. 2017).

Here, we present two new single-year ^{14}C records with annual to biannual time resolution for the periods AD 692–790 and AD 966–1057. We compare our measurements with existing data and the IntCal13 curve (Reimer et al. 2013) in order to validate the quality of our data. We further present relevant statistics to report on the dendrochronology of the wood pieces used in this study and the accelerator performance of the Aarhus AMS Centre (AARAMS) at Aarhus University, Denmark.

METHODS

Oak tree samples (*Quercus* sp.) from four locations in Denmark were collected and dendrochronologically dated by the tree-ring laboratory at the Danish National Museum. All tree-ring records were dendrochronologically matched with the oak master curves for West Denmark, Zealand, and Schleswig-Holstein using the program DENDRO for Windows (Tyers 1999) that relies on the methods outlined by Baillie and Pilcher (1973). The investigated pieces of wood originate from four different wood samples (Table 1). Ring widths for the wood records used in this study are listed in the supplementary table (Table S1).

All tree rings were separated into early (EW) and late wood (LW) fractions whenever possible. For the years where early and late wood could not be separated, the measurements are based on whole wood (WW) instead of late wood, which otherwise is used for all samples. The time resolution of the two datasets is predominantly biannual. Each data point associated with a year is based on at least two measurements in order to enhance the accuracy and precision. Whenever there was insufficient material to perform at least two measurements for the year of interest, one sample for the particular year and the subsequent year were measured.

α-cellulose was extracted from all wood samples using a combination of the methods proposed by Loader et al. (1997) and Southon and Magana (2010). The wood samples were bleached at 70°C with 1M sodium chlorite ($NaClO_2$), acidified with 1M hydrochloric acid (HCl), then treated at room temperature with 17% sodium hydroxide (NaOH) to dissolve hemicellulose. Lastly, they were treated with 1M hydrochloric acid at room temperature to remove any contamination from atmospheric CO_2. Subsequently, the α-cellulose was sealed in glass tubes containing copper oxide (CuO) and combusted to CO_2 at 900°C, cryogenically purified, and then reduced to graphite using hydrogen and iron as catalyst. All samples were analysed using the 1MV High Voltage Engineering accelerator mass spectrometer system at the Aarhus AMS Centre, Aarhus University, Denmark (Olsen et al. 2017). [14]C ages are reported as conventional ^{14}C ages in ^{14}C yr BP based on the measured ^{14}C/^{12}C ratio corrected for both natural and process isotopic fractionation by normalizing the result to the standard $\delta^{13}C$ value of –25‰ VPDB using the ^{13}C/^{12}C ratios measured during AMS analysis (Stuiver and Polach, 1977). The ^{14}C ages are further converted to decay-corrected $\Delta^{14}C$ values using

$$\Delta^{14}C = \left\lceil \frac{exp(-t_{C14}/8033)}{exp(-t_{cal}/8266)} - 1 \right\rceil \times 1000‰$$

where t_{C14} is the ^{14}C age and t_{cal} the calendar age. All ^{14}C data are presented in Table 2.

RESULTS AND DISCUSSION

The pieces of wood cover the two periods AD 692–790 and AD 966–1057 (hereafter referred to as the AD 750 and AD 1000 dataset, respectively). Tree-ring widths associated with each piece of wood used in this study are shown along with the master curve in Figure 1. Only a limited part of each wood piece was used for ^{14}C measurements where tree rings were sufficiently preserved and broad enough for separation of late and early wood (Tables 1 and S1). Student-t test values of matches between the wood pieces and the dendrochronological master curve of West Denmark are 11.0, 5.7, 4.4 and 6.4 for Ravning Enge (RE1), Østergård (ØG), Haderslev Fjord (HF) and Mojbøl (MOJ) respectively. The best Student-t match for Gråbrødre Kloster (GBK) was the Zealand master curve with a Student-t test value of 6.0 (Table 1).

The new single-year measurements generally agree with the main structures in the IntCal13 curve, but these also add new detailed structures to the curve (e.g. around AD 700, 762, 1014 and 1040) (Figure 2). The new datasets capture two rapid solar cosmic-ray events in AD 775 and AD 993. In the AD 750 dataset, an offset towards lower $\Delta^{14}C$ values exists between the new data and the IntCal13 curve between AD 725 and 760 and just before the onset of the AD 775 event. The mean Gaussian filters of the measurements in Figures 2 and 3 are based on calculated weighted means (weighted by error) and show the general fluctuations of the new data. The z-scores of replicate measurements (n = 196) for the combined AD 750 and AD 1000 dataset follow a normal distribution with a mean value of –0.02 ± 0.86. The replicate z-scores pass a reduced χ^2 test ($0.7 \leq 1.2$), indicating that we are able to reproduce measurements from the same year. Although the total number of replicates passes a χ^2 test, some disagreements between several replicate years still persist (AD 724, 766, 781, 1021, 1045 and 1055, Table 2), highlighting the advantage of measuring more than one sample for each year that is analyzed. Four international comparison standards have been used to confirm the accuracy during analysis: IAEA-C3 ($F^{14}C = 1.2959 \pm 0.003$, n = 111, $F^{14}C_{TRUE} = 1.2941 \pm 0.0006$), IAEA-C7 ($F^{14}C = 0.4954 \pm 0.0002$, n = 157, $F^{14}C_{TRUE} = 0.4953 \pm 0.0012$), IAEA-C8 ($F^{14}C = 0.1503 \pm 0.0001$, n = 158, $F^{14}C_{TRUE} = 0.1503 \pm 0.0017$) and FIRI-D ($F^{14}C = 0.5695 \pm 0.0002$, n = 194, $F^{14}C_{TRUE} = 0.5705 \pm 0.0002$). Whereas IAEA-C7 and C8 are agreeing well with the true $F^{14}C$ value, the IAEA-C3 is too young and the FIRI-D is slightly too old. The reason for the IAEA-C3 discrepancy is unknown, whereas as we suspect that the pretreatment method may explain the FIRI-D discrepancy. All FIRI-D samples are pretreated using our standard acid-base-acid pretreatment, and two recent analysis of FIRI-D on extracted cellulose provided an $F^{14}C$ value of 0.5704 ± 0.0011, in perfect agreement with the expected FIRI D $F^{14}C$ value. However, more data is required in order to be able to conclude whether or not the pretreatment may explain the FIRI-D discrepancy. Furthermore, samples from two broad rings have provided enough material for several ^{14}C analyses, which have been measured in different measurement batches.

Samples AAR-27091 and AAR–27770 have been analyzed in 6 (one outlier) and 4 batches, respectively, providing evidence for good reproducibility for the duration of the ^{14}C analysis of tree-ring batches (Table 2). The dendrochronological dating of the wood piece RE1 is verified by the AD 775 event, as the timing of the event recorded in this study is in full agreement with existing ^{14}C records from all over the world (Figure 3A). The period spanned by AD 980–1006 in the AD 1000 dataset is plotted along with published ^{14}C data by Fogtmann-Schulz et al. (2017) in Figure 4. The wood piece used in the study by Fogtmann-Schulz et al. (2017) was dendrochronologically dated by the Danish National

Table 1 Information on wood records used in this study.

Wood record	Short name	Wood number	Used years (AD)	Used rings	Latitude (°N)	Longitude (°E)	Student-t	Reference
Ravning Enge	RE1	6011_149	692–790	16–114	55.671166	9.346313	11.0[a] (6.2)[b]	Baittinger (2009)
Gråbrødre Kloster	GBK	60740109	966–990	21–45	56.460082	10.038167	6.0[c] (4.9)[a]	Eriksen (1998)
Østergård	ØG	50700289	980–1018	5–43	55.176060	9.171600	5.7[a] (3.6)[b]	Eriksen (1999)
Haderslev Fjord	HF	50050219	1010–1057	20–67	55.284980	9.658247	7.0[a] (5.4)[b]	Bonde (1992)
Mojbøl	MOJ	50851229	979–1007	6–34	55.297857	9.174393	6.4[a] (4.8)[b]	Eriksen (2004)

[a]West Denmark master chronology (National Museum of Denmark, Environmental Archaeology and Materials Science).
[b]Schleswig-Holstein master chronology (University of Hamburg, Department of Wood Science).
[c]Sjælland master chronology (National Museum of Denmark, Environmental Archaeology and Materials Science).

Table 2 ^{14}C tree-ring analysis: ^{14}C ages of late-wood (LW) or whole-wood (WW) rings presented in this study. The ^{14}C Age$_{mean}$ column provides the weighted mean ^{14}C age with a reduced χ^2 test (95.4% confidence level) given as X≤ Y. The χ^2 is passed if and only if X≤Y (Bevington and Robinson 2003). The deviation in terms of standard deviations (dev σ) is calculated as (^{14}C Age – ^{14}C Age$_{mean}$)/σ[^{14}C Age].

Lab ID	Name	Year (AD)	^{14}C Age (^{14}C yr BP)	dev σ	^{14}C Age$_{mean}$ (^{14}C yr BP)	Δ^{14}C (‰)	δ^{13}C$_{AMS}$ (‰ VPDB)
AAR-27737	RE1 692 LW	692	1257 ±19	–0.3	1262 ±12	–4.9 ±1.5	–23 ±1
			1267 ±16	0.3	(0.2≤3.8)		
AAR-27736	RE1 693 LW	693	1284 ±15		1284 ±15	–7.8 ±1.9	–26 ±1
AAR-27735	RE1 694 LW	694	1257 ±16	–1.0	1273 ±11	–6.5 ±1.4	–20 ±1
			1288 ±16	1.0	(1.9≤3.8)		
AAR-27734	RE1 695 LW	695	1319 ±17		1319 ±17	–12.3 ±2.1	–24 ±2
AAR-27733	RE1 696 LW	696	1246 ±15	0.6	1237 ±12	–2.2 ±1.5	–20 ±1
			1221 ±19	–0.8	(1.0≤3.8)		
AAR-27732	RE1 697 LW	697	1306 ±16		1306 ±16	–10.9 ±2.0	–27 ±1
AAR-27731	RE1 698 LW	698	1312 ±14	0.0	1312 ±14	–11.8 ±1.7	–23 ±1
			1185 ±16*	–8.0			
AAR-27730	RE1 699 LW	699	1264 ±16		1264 ±16	–6.0 ±2.0	–27 ±1
AAR-27729	RE1 700 LW	700	1304 ±16	1.8	1276 ±19	–7.5 ±2.4	–24 ±1
			1247 ±16	–1.8	(6.7≤3.8)		
AAR-27728	RE1 701 LW	701	1286 ±15		1286 ±15	–9.0 ±1.8	–21 ±1
AAR-27727	RE1 702 LW	702	1310 ±16	1.0	1294 ±11	–10.0 ±1.4	–22 ±1
			1278 ±16	–1.0	(2.0≤3.8)		
AAR-27725	RE1 704 LW	704	1289 ±16	–0.5	1297 ±11	–10.7 ±1.4	–23 ±1
			1306 ±17	0.5	(0.5≤3.8)		
AAR-27723	RE1 706 LW	706	1276 ±13	0.9	1265 ±10	–6.9 ±1.3	–20 ±1
			1241 ±18	–1.3	(2.4≤3.8)		
AAR-27721	RE1 708 LW	708	1226 ±17	0.7	1214 ±11	–0.9 ±1.4	–27 ±1
			1204 ±16	–0.7	(0.9≤3.8)		
AAR-27719	RE1 710 LW	710	1234 ±15	0.5	1227 ±11	–2.8 ±1.4	–24 ±1
			1220 ±16	–0.5	(0.5≤3.8)		

(*Continued*)

Table 2 (*Continued*)

Lab ID	Name	Year (AD)	^{14}C Age (^{14}C yr BP)	dev σ	^{14}C Age$_{mean}$ (^{14}C yr BP)	Δ^{14}C (‰)	δ^{13}C$_{AMS}$ (‰ VPDB)
AAR-27716	RE1 712 WW	712	1273 ±15	0.5	1265 ±11	–7.7 ±1.3	–24 ±1
			1257 ±15	–0.5	(0.5≤3.8)		
AAR-27125	RE1 714 LW	714	1280 ±14	0.1	1278 ±11	–9.6 ±1.3	–25 ±1
			1277 ±17	–0.1	(0.0≤3.8)		
AAR-27123	RE1 716 LW	716	1253 ±13	0.5	1246 ±11	–5.8 ±1.4	–22 ±1
			1226 ±22	–0.9	(1.1≤3.8)		
AAR-27122	RE1 718 LW	718	1261 ±14	0.4	1256 ±11	–7.3 ±1.4	–28 ±1
			1247 ±18	–0.5	(0.4≤3.8)		
AAR-27132	RE1 720 WW	720	1249 ±16		1249 ±16	–6.6 ±2.0	–23 ±1
AAR-27119	RE1 722 LW	722	1260 ±23	0.5	1247 ±12	–6.7 ±1.5	–23 ±1
			1242 ±14	–0.3	(0.4≤3.8)		
AAR-27117	RE1 724 LW	724	1264 ±15	0.0	1264 ±15	–9.0 ±1.8	–27 ±1
			1318 ±16*	3.5			
AAR-27115	RE1 726 LW	726	1239 ±15	–0.1	1240 ±11	–6.3 ±1.4	–29 ±1
			1241 ±17	0.1	(0.0≤3.8)		
AAR-27131	RE1 728 WW	728	1280 ±17		1280 ±17	–11.5 ±2.1	–22 ±1
AAR-27129	RE1 730 WW	730	1308 ±18		1308 ±18	–15.1 ±2.2	–28 ±1
AAR-27113	RE1 732 LW	732	1303 ±15	0.8	1291 ±10	–13.3 ±1.3	–23 ±1
			1279 ±15	–0.8	(1.3≤3.8)		
AAR-27112	RE1 734 LW	734	1287 ±15	0.8	1275 ±12	–11.6 ±1.4	–28 ±1
			1259 ±18	–0.9	(1.4≤3.8)		
AAR-27110	RE1 736 LW	736	1275 ±15	–0.1	1276 ±11	–11.9 ±1.3	–28 ±1
			1277 ±15	0.1	(0.0≤3.8)		
AAR-27108	RE1 738 LW	738	1298 ±20	0.6	1285 ±12	–13.3 ±1.5	–28 ±1
			1279 ±15	–0.4	(0.6≤3.8)		
AAR-27106	RE1 740 LW	740	1301 ±15	0.3	1298 ±12	–15.0 ±1.5	–27 ±1
			1291 ±20	–0.3	(0.2≤3.8)		
AAR-27104	RE1 742 LW	742	1309 ±18	1.6	1280 ±14	–13.1 ±1.7	–30 ±1
			1258 ±16	–1.4	(4.4≤3.8)		

Table 2 (*Continued*)

Lab ID	Name	Year (AD)	^{14}C Age (^{14}C yr BP)	dev σ	^{14}C Age$_{mean}$ (^{14}C yr BP)	Δ^{14}C (‰)	δ^{13}C$_{AMS}$ (‰ VPDB)
AAR-27102	RE1 744 LW	744	1305 ±17	0.1	1304 ±11	−16.3 ±1.4	−31 ±1
			1303 ±15	−0.1	(0.0≤3.8)		
AAR-27100	RE1 746 LW	746	1300 ±14	1.0	1285 ±10	−14.3 ±1.3	−23 ±1
			1268 ±15	−1.1	(2.2≤3.8)		
AAR-27098	RE1 748 LW	748	1314 ±16	0.5	1307 ±11	−17.1 ±1.3	−27 ±1
			1300 ±15	−0.4	(0.4≤3.8)		
AAR-27096	RE1 750 LW	750	1335 ±15	1.5	1312 ±13	−18.0 ±1.5	−27 ±1
			1289 ±15	−1.5	(4.5≤3.8)		
AAR-27094	RE1 752 LW	752	1308 ±16	0.4	1302 ±11	−17.0 ±1.3	−26 ±1
			1295 ±15	−0.4	(0.3≤3.8)		
AAR-27092	RE1 754 LW	754	1314 ±15	0.1	1313 ±11	−18.6 ±1.4	−25 ±1
			1312 ±16	−0.1	(0.0≤3.8)		
AAR-27091	RE1 755 LW	755	1312 ±15	−0.7	1322 ±7	−19.8 ±0.9	−24 ±1
			1327 ±23	0.2	(0.4≤2.4)		
			1321 ±14	−0.1			
			1266 ±14*	−4.0			
			1338 ±16	1.0			
			1318 ±15	−0.3			
AAR-27090	RE1 756 LW	756	1318 ±15		1318 ±15	−19.4 ±1.8	−27 ±1
AAR-27088	RE1 758 LW	758	1324 ±19	0.6	1313 ±9	−19.0 ±1.1	−25 ±1
			1305 ±14	−0.6	(0.3≤3.0)		
			1315 ±15	0.1			
AAR-24871	RE1 759 LW	759	1267 ±20		1267 ±20	−13.5 ±2.5	−27 ±1
AAR-24873	RE1 760 LW	760	1288 ±19	1.3	1263 ±21	−13.1 ±2.5	−27 ±1
			1215 ±26	−1.8	(5.2≤3.8)		
AAR-24875	RE1 761 LW	761	1321 ±30	1.2	1284 ±21	−15.9 ±2.5	−25 ±1
			1252 ±28	−1.1	(2.7≤3.8)		
AAR-24877	RE1 762 LW	762	1255 ±26	−1.5	1295 ±15	−17.3 ±1.8	−22 ±1
			1315 ±18	1.1	(3.5≤3.8)		

(*Continued*)

Table 2 (*Continued*)

Lab ID	Name	Year (AD)	^{14}C Age (^{14}C yr BP)	dev σ	^{14}C Age$_{mean}$ (^{14}C yr BP)	Δ^{14}C (‰)	δ^{13}C$_{AMS}$ (‰ VPDB)
AAR-24879	RE1 763 LW	763	1267 ±19	0.1	1266 ±17	–13.9 ±2.1	–28 ±1
			1259 ±46	–0.2	(0.0≤3.8)		
AAR-24881	RE1 764 LW	764	1276 ±17	0.5	1267 ±14	–14.2 ±1.8	–28 ±1
			1247 ±27	–0.8	(0.8≤3.8)		
AAR-24883	RE1 765 LW	765	1271 ±19	–1.4	1298 ±16	–18.0 ±2.0	–21 ±1
			1330 ±20	1.6	(4.6≤3.8)		
AAR-24885	RE1 766 LW	766	1297 ±20	1.3	1270 ±20	–14.7 ±2.4	–28 ±1
			1226 ±26	–1.7	(4.8≤3.8)		
AAR-24887	RE1 767 LW	767	1364 ±24	0.5	1352 ±14	–24.9 ±1.7	–23 ±1
			1346 ±17	–0.4	(0.4≤3.8)		
AAR-24889	RE1 768 LW	768	1307 ±21	1.2	1282 ±16	–16.5 ±2.0	–29 ±1
			1247 ±25	–1.4	(3.4≤3.8)		
AAR-24891	RE1 769 LW	769	1275 ±19		1275 ±19	–15.7 ±2.3	–19 ±1
AAR-24893	RE1 770 LW	770	1281 ±15	–1.1	1298 ±13	–18.7 ±1.6	–25 ±1
			1335 ±22	1.7	(4.0≤3.8)		
AAR-24895	RE1 771 LW	771	1271 ±22		1271 ±22	–15.4 ±2.7	–25 ±1
AAR-24897	RE1 772 LW	772	1273 ±19	–1.2	1296 ±13	–18.7 ±1.6	–28 ±1
			1318 ±18	1.2	(2.9≤3.8)		
AAR-24899	RE1 773 LW	773	1321 ±25	0.3	1314 ±20	–20.9 ±2.4	–27 ±1
			1301 ±33	–0.4	(0.2≤3.8)		
AAR-24901	RE1 774 LW	774	1190 ±22	–0.4	1199 ±16	–6.9 ±2.0	–21 ±1
			1210 ±24	0.4	(0.4≤3.8)		
AAR-24903	RE1 775 LW	775	1108 ±23	–0.3	1115 ±14	3.4 ±1.7	–23 ±1
			1118 ±17	0.2	(0.1≤3.8)		
AAR-24905	RE1 776 LW	776	1135 ±15		1135 ±15	0.7 ±1.8	–25 ±1
AAR-24907	RE1 777 LW	777	1132 ±26	0.7	1113 ±18	3.4 ±2.2	–24 ±1
			1096 ±24	–0.7	(1.1≤3.8)		
AAR-24909	RE1 778 LW	778	1097 ±24		1097 ±24	5.3 ±3.0	–24 ±1

Table 2 (*Continued*)

Lab ID	Name	Year (AD)	^{14}C Age (^{14}C yr BP)	dev σ	^{14}C Age$_{mean}$ (^{14}C yr BP)	Δ^{14}C (‰)	δ^{13}C$_{AMS}$ (‰ VPDB)
AAR-24911	RE1 779 LW	779	1170 ±31	0.5	1155 ±19	–2.1 ±2.4	–28 ±1
			1146 ±24	–0.4	(0.4≤3.8)		
AAR-24913	RE1 780 LW	780	1195 ±26		1195 ±26	–7.2 ±3.3	–29 ±1
AAR-24915	RE1 781 LW	781	1188 ±22	1.3	1160 ±20	–3.0 ±2.5	–23 ±1
			1110 ±30	–1.7	(4.4≤3.8)		
AAR-24917	RE1 782 LW	782	1165 ±20		1165 ±20	–3.7 ±2.4	–22 ±1
AAR-24919	RE1 783 LW	783	1145 ±19	0.2	1141 ±15	–0.9 ±1.9	–24 ±1
			1135 ±26	–0.2	(0.1≤3.8)		
AAR-24921	RE1 784 LW	784	1148 ±33		1148 ±33	–1.8 ±4.1	–29 ±1
AAR-24923	RE1 785 LW	785	1243 ±24*				–30 ±1
AAR-24927	RE1 787 LW	787	1161 ±19		1161 ±19	–3.8 ±2.3	–28 ±1
AAR-24929	RE1 788 LW	788	1184 ±15	0.3	1179 ±13	–6.2 ±1.6	–28 ±1
			1167 ±24	–0.5	(0.4≤3.8)		
AAR-24931	RE1 789 LW	789	1201 ±15	–0.2	1204 ±14	–9.3 ±1.7	–25 ±1
			1215 ±32	0.4	(0.2≤3.8)		
AAR-24933	RE1 790 LW	790	1223 ±19		1223 ±19	–11.9 ±2.4	–30 ±1
AAR-26479	GBK 966 LW	966	1082 ±22		1082 ±22	–15.5 ±2.7	–29 ±1
AAR-26480	GBK 967 LW	967	1079 ±19		1079 ±19	–15.3 ±2.3	–25 ±1
AAR-26481	GBK 968 LW	968	1127 ±19	0.7	1114 ±13	–19.7 ±1.5	–27 ±1
			1104 ±17	–0.6	(0.8≤3.8)		
AAR-26482	GBK 969 LW	969	1118 ±25		1118 ±25	–20.2 ±3.0	–29 ±1
AAR-26483	GBK 970 LW	970	1105 ±22		1105 ±22	–18.8 ±2.7	–28 ±1
AAR-26485	GBK 972 LW	972	1089 ±18	–0.5	1097 ±11	–18.1 ±1.4	–25 ±1
			1103 ±15	0.4	(0.4≤3.8)		
AAR-26487	GBK 974 LW	974	1106 ±20	0.2	1102 ±12	–19.0 ±1.4	–28 ±1
			1100 ±15	–0.1	(0.0≤3.8)		
AAR-26489	GBK 976 LW	976	1078 ±21	–1.3	1107 ±12	–19.7 ±1.5	–25 ±1
			1121 ±15	1.0	(2.7≤3.8)		

(*Continued*)

Table 2 (*Continued*)

Lab ID	Name	Year (AD)	^{14}C Age (^{14}C yr BP)	dev σ	^{14}C Age$_{mean}$ (^{14}C yr BP)	Δ^{14}C (‰)	δ^{13}C$_{AMS}$ (‰ VPDB)
AAR-26491	GBK 978 LW	978	1087 ±22		1087 ±22	−17.5 ±2.7	−29 ±1
AAR-26492	GBK 979 LW	979	1050 ±21	−1.2	1076 ±14	−16.4 ±1.8	−27 ±1
			1099 ±20	1.2	(2.9≤3.8)		
AAR-27770	ØG 980 LW	980	1102 ±18	0.7	1089 ±8(1.2≤2.6)	−18.1 ±0.9	−24 ±1
			1102 ±16	0.8			
			1068 ±14	−1.5			
			1093 ±15	0.2			
AAR-26494	GBK 981 LW	981	1124 ±21	0.1	1122 ±15	−22.1 ±1.9	−27 ±1
			1119 ±23	−0.1	(0.0≤3.8)		
AAR-27772	ØG 982 LW	982	1090 ±25		1090 ±25	−18.4 ±3.1	−24 ±1
AAR-26496	GBK 983 LW	983	1012 ±18*	−4.2	1089 ±15	−18.4 ±1.9	−27 ±1
			1089 ±15	0.0			
AAR-27774	ØG 984 LW	984	1043 ±24		1043 ±24	−12.9 ±3.0	−17 ±1
AAR-26498	GBK 985 LW	985	1065 ±21	−0.1	1067 ±12	−15.9 ±1.5	−26 ±1
			1067 ±15	0.1	(0.0≤3.8)		
AAR-27776	ØG 986 LW	986	1006 ±22		1006 ±22	−8.6 ±2.7	−24 ±1
AAR-26500	GBK 987 LW	987	1067 ±19	−0.8	1081 ±12	−17.9 ±1.4	−29 ±1
			1091 ±15	0.6	(1.0≤3.8)		
AAR-26502	GBK 989 LW	989	1102 ±18		1102 ±18	−20.7 ±2.2	−27 ±1
AAR-26503	GBK 990 LW	990	1008 ±25		1008 ±25	−9.3 ±3.0	−21 ±1
AAR-27781	ØG 991 LW	991	1082 ±15	0.0	1081 ±12	−18.4 ±1.4	−25 ±1
			1080 ±20	−0.1	(0.0≤3.8)		
AAR-27782	ØG 992 LW	992	1086 ±16	−0.1	1087 ±12	−19.2 ±1.5	−25 ±1
			1088 ±19	0.1	(0.0≤3.8)		
AAR-27783	ØG 993 LW	993	994 ±21	0.3	987 ±12	−7.1 ±1.5	−26 ±1
			984 ±15	−0.2	(0.2≤3.8)		
AAR-27784	ØG 994 LW	994	1004 ±16	0.0	1004 ±16	−9.2 ±1.9	−27 ±1
			1045 ±14*	3.0			
AAR-27785	ØG 995 LW	995	1034 ±16	−0.3	1039 ±11	−13.7 ±1.4	−26 ±1
			1044 ±15	0.3	(0.2≤3.8)		

Table 2 (*Continued*)

Lab ID	Name	Year (AD)	¹⁴C Age (¹⁴C yr BP)	dev σ	¹⁴C Age$_{mean}$ (¹⁴C yr BP)	Δ¹⁴C (‰)	δ¹³C$_{AMS}$ (‰ VPDB)
AAR-27786	ØG 996 LW	996	1019 ±21		1019 ±21	–11.4 ±2.6	–28 ±1
AAR-27787	ØG 997 LW	997	1040 ±14		1040 ±14	–14.0 ±1.8	–25 ±1
AAR-27788	ØG 998 LW	998	1005 ±17		1005 ±17	–9.9 ±2.1	–26 ±1
AAR-27790	ØG 1000 LW	1000	1072 ±15	1.1	1054 ±11	–16.2 ±1.3	–23 ±1
			1038 ±15	–1.1	(2.6≤3.8)		
AAR-27792	ØG 1002 LW	1002	1066 ±16		1066 ±16	–17.9 ±1.9	–23 ±1
AAR-27794	ØG 1004 LW	1004	1057 ±17	0.2	1054 ±11	–16.6 ±1.4	–24 ±1
			1052 ±15	–0.1	(0.0≤3.8)		
AAR-27796	ØG 1006 LW	1006	1039 ±17		1039 ±17	–15.0 ±2.1	–26 ±1
AAR-27797	ØG 1007 LW	1007	1074 ±15		1074 ±15	–19.5 ±1.8	–22 ±1
AAR-27798	ØG 1008 LW	1008	1072 ±16	1.1	1054 ±12	–17.1 ±1.5	–25 ±1
			1029 ±19	–1.3	(2.9≤3.8)		
AAR-27800	ØG 1010 LW	1010	1033 ±20	–0.8	1048 ±10	–16.6 ±1.2	–24 ±1
AAR-27820	HF 1010 LW		1035 ±16	–0.8	(1.5≤3.0)		
AAR-27820	HF 1010 LW		1070 ±16	1.4			
AAR-27821	HF 1011 LW	1011	1065 ±15		1065 ±15	–18.8 ±1.9	–22 ±1
AAR-27802	ØG 1012 LW	1012	1033 ±22	–0.4	1043 ±12	–16.2 ±1.5	–22 ±1
AAR-27822	HF 1012 LW		1047 ±15	0.3	(0.3≤3.8)		
AAR-27803	ØG 1013 LW	1013	1005 ±25	–0.0	1005 ±15	–11.7 ±1.9	–29 ±1
AAR-27823	HF 1013 LW		1006 ±19	0.0	(0.0≤3.8)		
AAR-27804	ØG 1014 LW	1014	1022 ±19	0.4	1015 ±13	–13.0 ±1.6	–27 ±1
AAR-27824	HF 1014 LW		1009 ±17	–0.3	(0.3≤3.8)		
AAR-27825	HF 1015 LW	1015	1031 ±16		1031 ±16	–15.1 ±1.9	–27 ±1
AAR-27806	ØG 1016 LW	1016	1084 ±18	0.6	1072 ±10	–20.3 ±1.2	–27 ±1
AAR-27826	HF 1016 LW		1064 ±16	–0.5	(0.3≤3.0)		
AAR-27826	HF 1016 LW		1072 ±18	–0.0			
AAR-27827	HF 1017 LW	1017	1028 ±16	–0.1	1029 ±12	–15.2 ±1.4	–30 ±1
			1031 ±18	0.1	(0.0≤3.8)		

(*Continued*)

Table 2 (*Continued*)

Lab ID	Name	Year (AD)	^{14}C Age (^{14}C yr BP)	dev σ	^{14}C Age$_{mean}$ (^{14}C yr BP)	Δ^{14}C (‰)	δ^{13}C$_{AMS}$ (‰ VPDB)
AAR-27808	ØG 1018 LW	1018	1063 ±17	0.6	1053 ±12	–18.1 ±1.4	–26 ±1
AAR-27828	HF 1018 LW		1044 ±16	–0.5	(0.6≤3.8)		
AAR-27829	HF 1019 LW	1019	1000 ±15	–1.0	1015 ±11	–13.6 ±1.4	–18 ±1
			1035 ±17	1.2	(2.4≤3.8)		
AAR-27830	HF 1020 LW	1020	1085 ±15		1085 ±15	–22.3 ±1.8	–27 ±1
AAR-27831	HF 1021 LW	1021	973 ±18	–2.4	1015 ±29	–13.8 ±3.5	–21 ±1
			1045 ±15	2.0	(9.7≤3.8)		
AAR-27833	HF 1023 LW	1023	999 ±17	–0.6	1009 ±9	–13.4 ±1.2	–21 ±1
			1005 ±17	–0.3	(0.5≤3.0)		
			1022 ±16	0.8			
AAR-27835	HF 1025 LW	1025	978 ±22	–1.1	1002 ±15	–12.7 ±1.8	–21 ±1
			1020 ±19	0.9	(2.0≤3.8)		
AAR-27837	HF 1027 LW	1027	1017 ±16	0.4	1011 ±11	–14.1 ±1.3	–27 ±1
			1006 ±15	–0.3	(0.3≤3.8)		
AAR-27839	HF 1029 LW	1029	968 ±17	–0.8	982 ±13	–10.7 ±1.6	–29 ±1
			1002 ±21	1.0	(1.6≤3.8)		
AAR-27841	HF 1031 LW	1031	989 ±15	–0.4	994 ±10	–12.5 ±1.2	–20 ±1
			1004 ±22	0.4	(0.2≤3.0)		
			996 ±15	0.1			
AAR-27843	HF 1033 LW	1033	958 ±15	–0.7	968 ±11	–9.6 ±1.3	–28 ±1
			981 ±16	0.8	(1.1≤3.8)		
AAR-27845	HF 1035 LW	1035	949 ±22	–1.0	970 ±13	–10.1 ±1.6	–20 ±1
			981 ±15	0.7	(1.4≤3.8)		
AAR-27847	HF 1037 LW	1037	1000 ±18	1.7	971 ±11	–10.4 ±1.3	–28 ±1
			941 ±15	–2.0	(3.5≤3.0)		
			979 ±15	0.5			
AAR-27849	HF 1039 LW	1039	937 ±16	0.2	933 ±11	–5.9 ±1.4	–21 ±1
			930 ±16	–0.2	(0.1≤3.8)		

Table 2 (*Continued*)

Lab ID	Name	Year (AD)	^{14}C Age (^{14}C yr BP)	dev σ	^{14}C Age$_{mean}$ (^{14}C yr BP)	Δ^{14}C (‰)	δ^{13}C$_{AMS}$ (‰ VPDB)
AAR-27851	HF 1041 LW	1041	888 ±17	–1.3	909 ±12	–3.2 ±1.4	–22 ±1
			928 ±16	1.2	(3.0≤3.8)		
AAR-27853	HF 1043 LW	1043	913 ±21	–1.1	936 ±10	–6.8 ±1.2	–24 ±1
			941 ±14	0.4	(0.7≤3.0)		
			944 ±17	0.4			
AAR-27855	HF 1045 LW	1045	957 ±17	–0.9	973 ±9	–11.5 ±1.1	–22 ±1
			1000 ±15	1.9	(2.8≤3.0)		
			953 ±16	–1.2			
AAR-27857	HF 1047 LW	1047	943 ±16		943 ±16	–8.2 ±2.0	–23 ±1
AAR-27858	HF 1048 LW	1048	936 ±15		936 ±15	–7.4 ±1.8	–27 ±1
AAR-27859	HF 1049 LW	1049	931 ±27	–0.6	946 ±12	–8.7 ±1.5	–26 ±1
			950 ±14	0.3	(0.4≤3.8)		
AAR-27861	HF 1051 LW	1051	926 ±16	0.3	921 ±11	–5.9 ±1.4	–22 ±1
			916 ±16	–0.3	(0.2≤3.8)		
AAR-27863	HF 1053 LW	1053	902 ±18	–1.4	927 ±9	–6.9 ±1.1	–23 ±1
			943 ±14	1.1	(1.7≤3.0)		
			927 ±15	–0.0			
AAR-27865	HF 1055 LW	1055	847 ±24	–1.4	882 ±12	–1.5 ±1.5	–23 ±1
			894 ±14	0.8	(2.8≤3.8)		
AAR-27867	HF 1057 LW	1057	914 ±16	–0.8	927 ±9	–7.3 ±1.1	–23 ±1
			940 ±14	1.0	(0.8≤3.0)		
			922 ±16	–0.3			
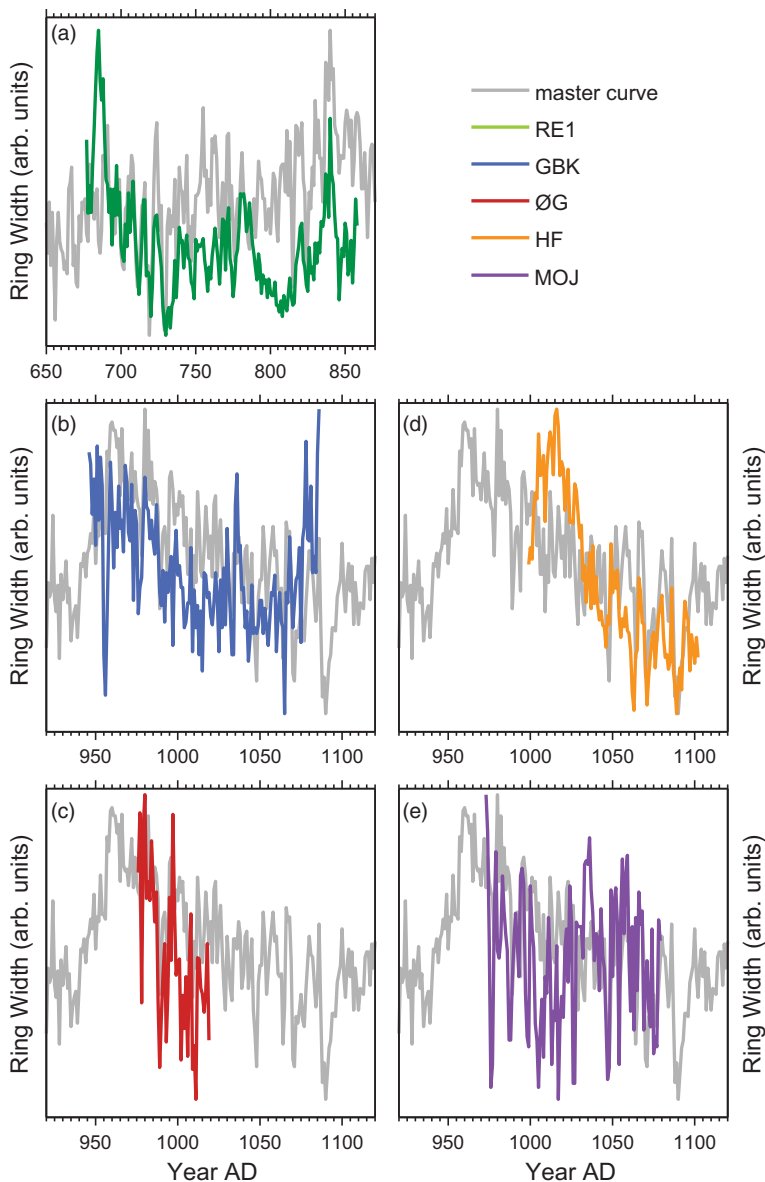
Figure 1   Measured ring widths of the pieces of wood used in this study. Indices are abbreviations of the location of each wood piece. RE1: Ravning Enge (green), GBK: Gråbrødre Kloster (blue), ØG: Østergård (red), HF: Haderslev Fjord (yellow) and MOJ: Mojbøl (purple). Black line is the master curve of West Denmark used for the dendrochronological dating. (Please see electronic version for color figures.)

Museum and prepared and analyzed at AARAMS like the wood pieces used in this study. Some disagreements between the AD 1000 dataset of this study and the data by Fogtmann-Schulz et al. (2017) are apparent for the years AD 1001–1006. In this period, the measurements by Fogtmann-Schulz et al. (2017) are based on single measurements of whole and late wood material, while the new data presented in this study are based on two
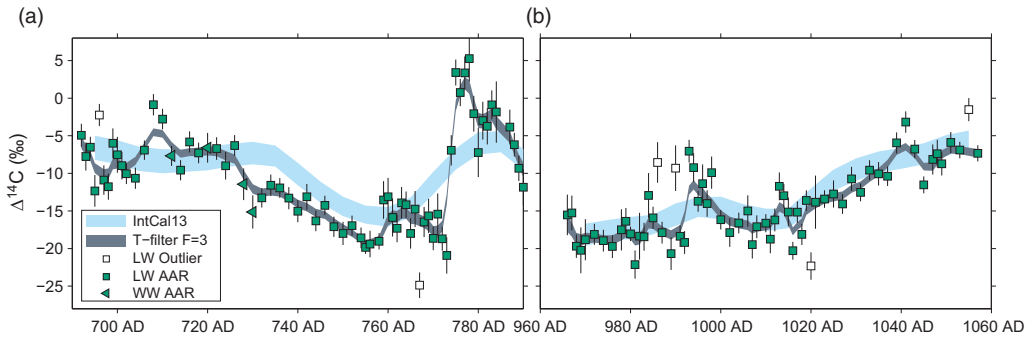
Figure 2 Combined annual/biannual $\Delta^{14}C$ values plotted together with the IntCal13 calibration curve (Reimer et al 2013). The grey curve is constructed using a running Gaussian mean filter of length 3 and is shown as guide for comparison with IntCal13.
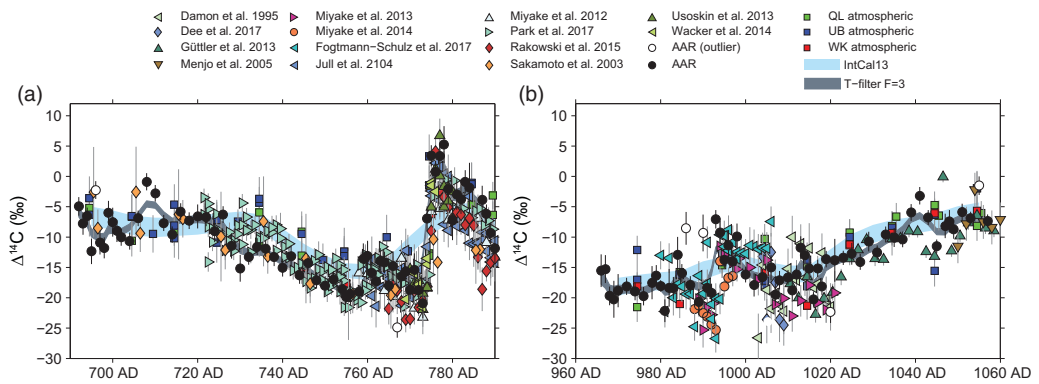
Figure 3 Weighted means and Gaussian mean filter of data from this study (black dots and grey curve) along with the IntCal13 curve (blue curve) and published data.
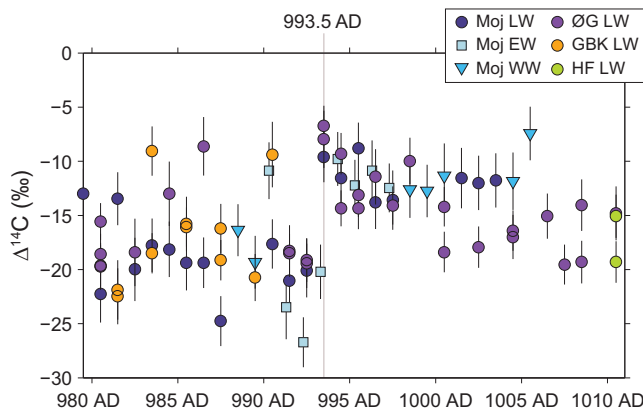
Figure 4 Weighted means of data from this study along with EW, LW and WW data published by Fogtmann-Schulz et al. (2017) across the AD 992/993 event.

measurements of late wood per reported year. The new data presented here appear to agree better with existing data for this period, and we therefore consider them more accurate than the data presented by Fogtmann-Schulz et al. (2017) for the years AD 1001–1006 (Figure 3B). A rather striking difference between the AD 1000 dataset and published data by Fogtmann-Schulz et al. (2017) concerns the occurrence of the AD 994 cosmic-ray event. The data presented by Fogtmann-Schulz et al. (2017) suggest the event occurred after the formation of early wood in AD 994 (i.e. in agreement with published data by Miyake et al. [2013, 2014]), whereas the AD 1000 dataset suggests the event took place between the late wood fractions in AD 992/993, i.e. one year earlier than proposed by Miyake et al. (2013, 2014) and Fogtmann-Schulz et al. (2017). In the period between AD 991 and 995, the AD 1000 dataset is based on two measurements of the late wood fraction, i.e. the most robust wood fraction for ^{14}C measurements (Kudsk et al. 2018). This discrepancy concerning the timing of the AD 994 event prompted us to scrutinize our laboratory methods and procedures as well as the dendrochronological age constraints. Careful remeasuring of the ring widths of the MOJ and ØG wood pieces showed that the dendrochronological ages of the MOJ record were displaced by –1 year. Thus, although the overall conclusions of Fogtmann-Schulz et al. (2017) remain valid, the timing of the event was one year too young. The updated information on the MOJ wood records has therefore been added to the present paper (Tables 1 and S1). Based on the corrected dendrochronological ages for the MOJ wood records, and the combined evidence from the two wood records (MOJ and ØG), we conclude that the cosmic-ray event took place during the summer of AD 993 (Figures 3 and 4).

The two new datasets presented in this study are shown in Figure 3 along with published tree-ring data in the literature. Whenever the published data are based on wood samples that cover more than one year, the age of the midpoint of the time span is used (e.g. for the published IntCal13 data (10-yr blocks), Sakamoto et al. 2003 (10-yr blocks), Güttler et al. (2013) (2-yr blocks)). The differences between the two new ^{14}C records presented here and published tree-ring data are generally small. The detailed structures found in the new AD 750 dataset around AD 690–720 agree well the 10-yr data blocks of Sakamoto et al. (2003). In the AD 750 dataset, we observe offsets toward lower values compared to IntCal13 in the period between AD 725 and 760. This offset is in agreement with the data published by Sakamoto et al. (2003) and Park et al. (2017) which both show a similar offset compared to the IntCal13. However, the new data presented here have slightly lower values compared to those of Park et al. (2017) but fit well with published data for the AD 775 event.

The pattern in the new AD 1000 dataset spanning the AD 994 event fits well with the existing data published by Miyake et al. (2013, 2014), which shows a similar decrease in ^{14}C after the cosmic-ray event. The relatively good agreement between the AD 1000 dataset and published data continue between AD 1000 and 1025, although the published data show that some discrepancies exist among the various datasets between AD 1040 and 1050, where they almost show opposite patterns. The new data are also in good agreement with data by Damon et al. (1995), particularly around the peak at AD 1015. Between AD 1025 and 1040, the new data are consistent with the data published by Güttler et al. (2013), but some discrepancies exist between the two datasets between AD 1040 and 1050, where they almost show opposite patterns.

Several studies have searched for fingerprints of proximal supernova by producing annual ^{14}C records across years associated with known supernova explosions (Damon et al. 1995;

Menjo et al. 2005; Dee et al. 2017). So far, no clear excursions have yet been found in any ^{14}C record that could be linked to a past supernova explosion. Two supernova explosions are known to have occurred in AD 1006 and 1054, and these events are thus covered by the new AD 1000 dataset. Although an increase in the atmospheric ^{14}C content can be observed at AD 1055 (Figure 2), there are no clear indications of any of the two supernova explosions.

CONCLUSION

In this study, we present two new ^{14}C records based on single-year measurements of Danish oak. The two new records, which span the periods AD 692–790 and 966–1057, have an annual to biannual time resolution. Each data point presented in this study is based on two separate samples and two separate measurements. Statistics on replicate measurements indicate that our data are reproducible, which increases the robustness and reliability of the new data. The two new records span the two rapid cosmic-ray events in AD 775 and 994. The timing of the AD 775 event in the data presented here is in full agreement with the timing reported in the literature, but the AD 994 event occurred one year earlier compared to existing records. Careful reanalysis of the dendrochronology that underpins the annually resolved ^{14}C records based on Danish oak published here and in Fogtmann-Schulz et al. (2017) suggests unequivocally that the AD 994 event actually took place in the summer of AD 993. The new data presented here generally agree with the trends in the current international calibration curve, although with a minor offset between AD 725 and 760, an offset that is also observed in other published annually resolved ^{14}C records. Finally, to meet the criteria for data to be included in the next international calibration curve (e.g. ring widths, t-values and achieve numbers), we also present all relevant information concerning the wood material on which the new ^{14}C records are based.

ACKNOWLEDGMENTS

SUPPLEMENTARY INFORMATION

Tree-ring widths of the wood piece used in the study by Fogtmann-Schulz et al. (2017) (MOJ) have been applied in the supplementary table along with tree-ring widths of the wood pieces used in this study in order to make the information public. Dendrochronological information of the MOJ wood piece is given in Eriksen et al. (2004) (wood piece 50851229).

SUPPLEMENTARY MATERIAL

To view supplementary material for this article, please visit https://doi.org/10.1017/RDC. 2019.107

REFERENCES

Baillie M, Pilcher J. 1973. A simple cross-dating program for tree-ring research. Tree-Ring Bulletin 33:7–14.

Baittinger C. 2009. Præliminær dendrokronologisk undersøgelse II af træprøver fra Ravning Enge. Nationalmuseets Naturvidenskabelige Undersøgelser NNU rapport 3.

Bevington PR, Robinson DK. 2003. Data reduction and error analysis for the physical sciences. 3rd ed. Boston (MA): McGraw-Hill.

Bonde N. 1992. Dendrokronologisk undersøgelse af træprøver fra spærring i Haderslev Fjord Nationalmuseets Naturvidenskabelige Undersøgelser NNU rapport 14.

Damon PE, Kaimei D, Kocharov GE, Mikheeva IB, Peristykh AN. 1995. Radiocarbon production by the gamma-ray component of supernova explosions. Radiocarbon 37(2):599–604.

Dee M, Pope B, Miles D, Manning S, Miyake F. 2017. Supernovae and single-year anomalies in the atmospheric radiocarbon record. Radiocarbon 59(2):293–302.

Eriksen OH. 1998. Dendrokronologisk undersøgelse af træ fra udgravning ved Gråbrødre kloster, Randers. Dendrokronologisk Laboratorium NNU rapport 38.

Eriksen OH. 1999. "Østergård", Haderslev Amt. Dendrokronologisk Laboratorium NNU rapport 24.

Eriksen OH. 2004. Dendrokronologisk undersøgelse af træ fra vadested ved Mojbøl i Sønderjyllands amt. Nationalmuseets Naturvidenskabelige Undersøgelser NNU rapport 2.

Fogtmann-Schulz A, Østbø SM, Nielsen SGB, Olsen J, Karoff C, Knudsen MF. 2017. Cosmic ray event in 994 C.E. recorded in radiocarbon from Danish oak. Geophysical Research Letters 44:8621–8628.

Gray LJ, Beer J, Geller M, Haigh JD, Lockwood M, Matthes K, Cubasch U, Fleitmann D, Harrison G, Hood L, et al. 2010. Solar influence on climate. Reviews of Geophysics 48:RG4001.

Güttler D, Wacker L, Kromer B, Friedrich M, Synal H-A. 2013. Evidence of 11-year solar cycles in tree-rings from 1010 to 1110 AD – progress on high precision AMS measurements. Nuclear Instruments and Methods in Physics Research B 294:459–463.

Güttler D, Adolphi F, Beer J, Bleicher N, Boswijk G, Christl M, Hogg A, Palmer J, Vockenhuber C, Wacker L, Wunder J. 2015. Rapid increase in cosmogenic ^{14}C in AD 775 measured in New Zealand kauri trees indicates short-lived increase in ^{14}C production spanning both hemispheres. Earth and Planetary Science Letters 411:290–297.

Jacobsson P, Hamilton WD, Cook G, Crone A, Dunbar E, Kinch H, Naysmith P, Tripney B, Xu S. 2017. Refining the Hallstatt Plateau: short-term ^{14}C variability and small scale offsets in 50 consecutive single tree-rings from southwest Scotland dendro-dated to 510–460 BC. Radiocarbon 60(1):219–237.

Jull AJT, Panyushkina IP, Lange TE, Kukarskih VV, Myglan VS, Clark KJ, Salzer MW, Burr GS, Leavitt SW. 2014. Excursions in the ^{14}C record at AD 774–775 in tree rings from Russia and America. Geophysical Research Letters 41:3004–3010.

Jull AJT, Panyuskina I, Miyake F, Masuda K, Nakamura T, Mitsutani T, Lange TE, Cruz RJ, Baisan C, Janovic R, Varga T, Molnár M. 2018. More rapid ^{14}C excursions in the tree-ring record: a record of different kind of solar activity at about 800 BC? Radiocarbon 60(4):1237–1248.

Kudsk S, Olsen J, Nielsen L, Fogtmann-Schulz A, Knudsen M, Karoff C. 2018. What is the carbon origin of early-wood? Radiocarbon 60(5):1457–1464.

Loader NJ, Robertson I, Barker AC, Switsur VR, Waterhouse JS. 1997. An improved technique for the batch processing of small wholewood samples to α-cellulose. Chemical Geology 136:313–317.

Marshall P, Bayliss A, Farid S, Tyers C, Bronk Ramsey C, Cook G, Doğan T, Freeman SPHT, İlkmen E, Knowles T. 2018. 14C wiggle-matching of short tree-ring sequences from post-medieval buildings in England. Nuclear Instruments and Methods in Physics Research B. in press.

Menjo H, Miyahara H, Kuwana K, Masuda K, Nakamura T. 2005. Possibility of the detection of past supernova explosion by radiocarbon measurement. 29th International Cosmic Ray Conference Pune 2:357–360.

Miyake F, Nagaya K, Masuda K, Nakamura T. 2012. A signature of cosmic-ray increase in AD 774–775 from tree rings in Japan. Nature 486(7402):240–242.

Miyake F, Masuda K, Nakamura T. 2013. Another rapid event in the carbon-14 content of tree rings. Nature Communications 4.

Miyake F, Masuda K, Hakozaki M, Nakamura T, Tokanai F, Kato K, Kimura K, Mitsutani T. 2014. Verification of the Cosmic-Ray Event in AD 993–994 by using a Japanese Hinoki tree. Radiocarbon 56(3):1189–1194.

Miyake F, Jull AJT, Panyushkina IP, Wacker L, Salzer M, Baisen CH, Lange T, Cruz R, Masuda K, Nakamura T. 2017a. Large ^{14}C excursion in 5480 BC indicates and abnormal sun in the mid-Holocene. PNAS 114(5):881–884.

Miyake F, Masuda K, Nakamura T, Kimura K, Hakozaki M, Jull A, Lange TE, Cruz R, Panyushkina IP, Baisan C, Salzer MW. 2017b. Search for annual ^{14}C excursions in the past. Radiocarbon 59(2):315–320.

Olsen J, Tikhomirov D, Grosen C, Heinemeier J, Klein M. 2017. Radiocarbon analysis on the new AARAMS 1MV Tandetron. Radiocarbon 59(3):905–913.

Park J, Southon J, Fahrni S, Creasman PP, Mewaldt R. 2017. Relationship between solar activity and $\Delta^{14}C$ peaks in AD 775, AD 994, and 660 BC. Radiocarbon 59(4):1147–1156.

Pearson CL, Brewer PW, Brown D, Heaton TJ, Hodgins GWL, Jull AJT, Lange T, Salzer MW. 2018. Annual radiocarbon record indicates 16th century BCE date for the Thera eruption. Science Advances 4(8):eaar8241.

Rakowski AZ, Krąpiec M, Huels M, Pawlyta J, Dreves A, Meadows J., 2015. Increase of radiocarbon concentration in tree rings from Kujawy (SE Poland) around AD 774–775. Nuclear Instruments and Methods in Physics Research Section B: Beam Interactions with Materials and Atoms 361:564–8.

Reimer PJ, Bard E, Bayliss A, Beck JW, Blackwell PG, Bronk Ramsey C, Buck CE, Cheng H, Edwards RL, Friedrich M, et al. 2013. IntCal13 and Marine13 radiocarbon age calibration curves 0–50,000 years cal BP. Radiocarbon 55(4):1869–1887.

Sakamoto M, Imamura M, Van der Plicht J, Mitsutani T, Sahara M. 2003. Radiocarbon calibration for Japanese wood samples. Radiocarbon 45(1):81–89.

Sakamoto M, Hakozaki M, Nakao N, Nakatsuka T. 2017. Fine structure and reproducibility of radiocarbon ages of middle to early modern Japanese tree rings. Radiocarbon 59(6): 1907–1917.

Southon JR, Magana AL. 2010. A comparison of cellulose extraction and ABA pretreatment methods for AMS ^{14}C dating of ancient wood. Radiocarbon 52(3):1371–1379.

Stuiver M, Polach HA. 1977. Reporting of ^{14}C data. Radiocarbon 19(3):355–363.

Tyers I. 1999. DENDRO for Windows Program Guide. Sheffield, U.K.: University of Sheffield; ARCUS report 500.

Usoskin IG, Kromer B, Ludlow F, Beer J, Friedrich M, Kovaltso GA, Solanki SK, Wacker L. 2013. The AD 775 cosmic event revisited: the Sun is to blame. Astronomy & Astrophysics 552:L3.

Wacker L, Güttler D, Goll J, Hurni JP, Synal H-A, Walti N. 2014. Radiocarbon dating to a single year by means of rapid atmospheric ^{14}C changes. Radiocarbon 56(2):573–579.

Wang FY, Yu H, Zou YC, Dai ZG, Cheng KS. 2017. A rapid cosmic-ray increase in BC 3372–3371 from ancient buried tree-rings in China. Nature Communications 8:1487.